PROCEEDINGS OF SCIENCE

Four-loop relation between the $\overline{\rm MS}$ and on-shell quark mass

Peter Marquard
Deutsches Elektronen Synchrotron DESY, Platanenallee 6, 15738 Zeuthen, Germany
E-mail: peter.marquard@desy.de

Alexander V. Smirnov
Scientific Research Computing Center, Moscow State University, 119991, Moscow, Russia
E-mail: asmirnov80@gmail.com

Vladimir A. Smirnov
Skobeltsyn Institute of Nuclear Physics, Moscow State University, 119991, Moscow, Russia
E-mail: smirnov@theory.sinp.msu.ru

Matthias Steinhauser*
Institut für Theoretische Teilchenphysik, Karlsruhe Institute of Technology (KIT), 76128 Karlsruhe, Germany
E-mail: matthias.steinhauser@kit.edu

In this contribution we discuss the four-loop relation between the on-shell and $\overline{\rm MS}$ definition of heavy quark masses which is applied to the top, bottom and charm case. We also present relations between the $\overline{\rm MS}$ quark mass and various threshold mass definitions and discuss the uncertainty at next-to-next-to-next-to-leading order.

12th International Symposium on Radiative Corrections (Radcor 2015) and LoopFest XIV (Radiative Corrections for the LHC and Future Colliders)
15-19 June, 2015
UCLA Department of Physics & Astronomy Los Angeles, USA

*Speaker.

1. Introduction

In the Standard Model (and many of its extensions) quark masses enter as fundamental parameters m_q into the underlying Lagrange density. Once quantum corrections are considered one has to fix the precise definition of m_q. For heavy quarks a natural one is the on-shell definition where one requires that the quark propagator $S_q(q)$ has a pole for $q^2 = (M_q^{\rm OS})^2$. However, there are many situations where other definitions are more convenient. As an example we mention the decay rate of Higgs bosons to bottom quarks where, when expressed in terms of the $\overline{\rm MS}$ bottom quark mass evaluated at the appropriate scale, potentially large logarithms are automatically summed up. A further example is the threshold production of top quark pairs in electron-positron annihilation. For this process one has to adopt a properly constructed (so-called) threshold mass which, on the one hand, is of short-distance nature as the $\overline{\rm MS}$ mass. On the other hand, it has similar features as the on-shell mass. In particular, it has a physical definition at threshold.

It is important to have precise relations among the various mass definitions. In Ref. [1] four-loop corrections to the relation between the $\overline{\rm MS}$ and on-shell heavy quark definition has been computed. This result has been used to derive next-to-next-to-next-to-leading order ($\rm N^3LO$) relations among the $\overline{\rm MS}$ and the most popular threshold masses, namely the PS [2], 1S [3, 4, 5] and RS [6] masses.

The relation between the $\overline{\rm MS}$ (m) and the on-shell mass (M) is obtained by considering in a first step their relation to the bare mass, m_0:

$$m^0 = Z_m^{\overline{\rm MS}} m\,, \qquad m^0 = Z_m^{\rm OS} M\,. \tag{1.1}$$

Here, $Z_m^{\overline{\rm MS}}$ is known to five-loop order [7]. However, in our calculation, only the four-loop result is necessary [8, 9, 10]. $Z_m^{\rm OS}$ is computed from the scalar and vector contribution of the quark two-point function with on-shell external momentum via

$$Z_m^{\rm OS} \;=\; 1 + \Sigma_V(q^2 = M^2) + \Sigma_S(q^2 = M^2)\,. \tag{1.2}$$

One-, two- and three-loop results to $Z_m^{\rm OS}$ have been computed in Refs. [11], [12] and [13, 14, 15, 16], respectively. Four-loop result have recently been computed in Ref. [1].

By construction, the ratio of the two equations in (1.1) is finite which leads to

$$z_m(\mu) \;=\; \frac{m(\mu)}{M}\,. \tag{1.3}$$

It is convenient to cast the perturbative expansion in the form

$$z_m(\mu) \;=\; \sum_{n\geq 0} \left(\frac{\alpha_s}{\pi}\right)^n z_m^{(n)}\,, \tag{1.4}$$

with $z_m^{(0)} = 1$. In the next section we present results for z_m up to four-loop order and discuss the numerical effects for charm, bottom and top quarks. Afterwards we consider in Section 3 the relation between the $\overline{\rm MS}$ and various threshold masses. Section 4 contains our conclusions.

2. Four-loop $\overline{\rm MS}$-on-shell relation

For the computation of the fermion self energy we use an automated setup which generates all contributing amplitudes with the help of `qgraf` [17]. The output is transformed to `FORM3`-readable [18] input using `q2e` and `exp` [19, 20]. Afterwards projectors for the scalar and vector part are applied, traces are taken and the scalar products in the numerator are decomposed in propagator factors. This leads to several million different integrals encoded in functions with 14 different indices which belong to 100 different integral families.

The Laporta algorithm [21] is applied to each family using `FIRE5` [22] and `crusher` [23] which are written in `C++`. Then we use the code `tsort` [24], which is part of the latest `FIRE` version, to reveal relations between primary master integrals (following recipes of Ref. [25]) and end up with 386 four-loop massive on-shell propagator integrals, i.e. with $p^2 = M^2$.

Up to this point the whole calculation is analytic. However, at the moment not all master integrals could be evaluated analytically but only numerically using `FIESTA` [26, 27, 28] which leads to an accuracy of about five to six digits for the highest ε expansion term. For some integrals a two- or threefold Mellin Barnes representation could be derived which enabled us to obtain a precision of more than eight, in some cases even more than 20 digits.

For each integral which is evaluated numerically, each ε coefficient gets a separate uncertainty assigned. Since it results from a numerical Monte Carlo integration we interpret it as a standard deviation and combine the individual uncertainties in the final expression quadratically. Furthermore, we multiply the uncertainty in the final result for the $\overline{\rm MS}$ and on-shell relation by a factor five.

Note that we have performed the calculation allowing for a general gauge parameter ξ keeping terms up to order ξ^2 in the expression we give to the reduction routines. We have checked that ξ drops out after mass renormalization but before inserting the master integrals.

In the following we show the $\overline{\rm MS}$-on-shell relation in the form where the on-shell mass is computed from the $\overline{\rm MS}$ mass. We discuss the top, bottom and charm quark case and use as input the following $\overline{\rm MS}$ masses: $m_t \equiv m_t(m_t) = 163.643$ GeV, $m_b \equiv m_b(m_b) = 4.163$ GeV [29], and $m_c(3\ GeV) = 0.986$ GeV [29]. The corresponding values for the strong coupling are given by $\alpha_s^{(6)}(m_t) = 0.1088$, $\alpha_s^{(5)}(m_b) = 0.2268$, and $\alpha_s^{(4)}(3\,\text{GeV}) = 0.2560$. They have been computed from $\alpha_s^{(5)}(M_Z) = 0.1185$ [30] using `RunDec` [31, 32]. In the case of the charm quark we also provide results for $\mu = m_c$ using the input values $m_c \equiv m_c(m_c) = 1.279$ GeV and $\alpha_s^{(4)}(m_c) = 0.3923$. Note that the choice $\mu = 3$ GeV is preferable since it has the advantage that low renormalization scales $\mu \approx m_c$ are avoided. Our results read

$$\begin{aligned} M_t &= m_t \left(1 + 0.4244\,\alpha_s + 0.8345\,\alpha_s^2 + 2.375\,\alpha_s^3 + (8.49 \pm 0.25)\,\alpha_s^4\right) \\ &= 163.643 + 7.557 + 1.617 + 0.501 + 0.195 \pm 0.005 \text{ GeV}, \end{aligned} \tag{2.1}$$

$$\begin{aligned} M_b &= m_b \left(1 + 0.4244\,\alpha_s + 0.9401\,\alpha_s^2 + 3.045\,\alpha_s^3 + (12.57 \pm 0.38)\,\alpha_s^4\right) \\ &= 4.163 + 0.401 + 0.201 + 0.148 + 0.138 \pm 0.004 \text{ GeV}, \end{aligned} \tag{2.2}$$

$$\begin{aligned} M_c &= m_c(3\text{ GeV}) \left(1 + 1.133\,\alpha_s + 3.119\,\alpha_s^2 + 10.98\,\alpha_s^3 + (51.29 \pm 0.52)\,\alpha_s^4\right) \\ &= 0.986 + 0.286 + 0.202 + 0.182 + 0.217 \pm 0.002 \text{ GeV}, \end{aligned} \tag{2.3}$$

$$\begin{aligned} M_c &= m_c \left(1 + 0.4244\,\alpha_s + 1.0456\,\alpha_s^2 + 3.757\,\alpha_s^3 + (17.36 \pm 0.52)\,\alpha_s^4\right) \\ &= 1.279 + 0.213 + 0.206 + 0.290 + 0.526 \pm 0.016 \text{ GeV}. \end{aligned} \tag{2.4}$$

For the top quark the higher order corrections become successively smaller by a factor two to three leading to a four-loop correction term of about 200 MeV. This is the same order of magnitude as the intrinsic uncertainty of the $\overline{\rm MS}$-on-shell relation given by $\Lambda_{\rm QCD}$. The four-loop corrections are still smaller than the current uncertainty of the top quark form the TEVATRON and the LHC [33]. However, they are not negligible.

For the bottom and charm quark case the situation is completely different. No convergence is observed when increasing the loop order. In the case of the charm quark where $m_c(m_c)$ is chosen as a starting point one even observes a four-loop coefficient which is almost twice as large as the three-loop one.

From the above results one can conclude that the immediate application of the $\overline{\rm MS}$-on-shell relation is only meaningful for the top quark case. For the lighter quarks the on-shell mass parameter should be avoided. If necessary an appropriately chosen threshold mass should be used as we will discuss in the next section.

In the following we present for the top quark mass the inverted relation of Eq. (2.1) which reads[1]

$$\begin{aligned} m_t &= M_t \left(1 - 0.4244\,\alpha_s - 0.65441\,\alpha_s^2 - 1.944\,\alpha_s^3 - (7.23 \pm 0.22)\,\alpha_s^4\right) \\ &= 173.34 - 7.948 - 1.324 - 0.425 - 0.171 \pm 0.005 \text{ GeV}, \end{aligned} \tag{2.5}$$

where $M_t = 173.34$ GeV [33] and $\alpha_s^{(6)}(M_t) = 0.1080$ has been used. This equation can be used to compute $m_t(m_t)$ for a given value for the on-shell mass M_t.

3. Relation between $\overline{\rm MS}$ and threshold masses to N^{3}LO

In this section we present numerical results for the $\overline{\rm MS}$ quark masses using input values for the PS, 1S and RS threshold masses. In practical applications the latter are extracted from comparisons with experimental data. The derivation of the N^{3}LO relations is discussed in Ref. [1] following the prescriptions provided in the original references [2, 3, 4, 5, 6].

Table 1 shows results for the $\overline{\rm MS}$ top quark mass computed from the PS, 1S and RS threshold mass values given in the first and second row. Note that these values are chosen in such a way that in all three cases the same $\overline{\rm MS}$ mass is obtained after applying four-loop corrections, which facilitates the comparison. Note also, that in contrast to the corresponding table in Ref. [1] we choose for the factorization scale of the PS mass $\mu_f = 80$ GeV instead of $\mu_f = 20$ GeV. This is suggested by the N^{3}LO threshold analysis of $\sigma(e^+e^- \to t\bar{t})$ performed in Ref. [34]. The factorization scale for the RS mass is kept at $\mu_f = 20$ GeV.

In all three cases one observes a rapid convergence of the perturbative series. In fact, the NNLO term amounts to at most 210 MeV (1S mass), and at N^{3}LO at most 20 MeV (RS mass). After increasing the four-loop $\overline{\rm MS}$-on-shell term by 3%, which is the current uncertainty on the four-loop coefficient in Eq. (1.4), the mass values reduces by 6 MeV. Combining these two sources

[1] Note that the $\overline{\rm MS}$ value used in Eq. (2.1) has been obtained using Eq. (2.5) to three-loop accuracy.

input	$m^{\rm PS}=$	$m^{\rm 1S}=$	$m^{\rm RS}=$
#loops	168.204	172.227	171.215
1	164.311	165.045	164.847
2	163.713	163.861	163.853
3	163.625	163.651	163.663
4	163.643	163.643	163.643
4 ($\times$1.03)	163.637	163.637	163.637

Table 1: $m_t(m_t)$ in GeV computed from the PS, 1S and RS quark mass using LO to N^{3}LO accuracy. The numbers in the last line are obtained by taking into account the uncertainty of the four-loop coefficient, i.e., it is increased by 3%.

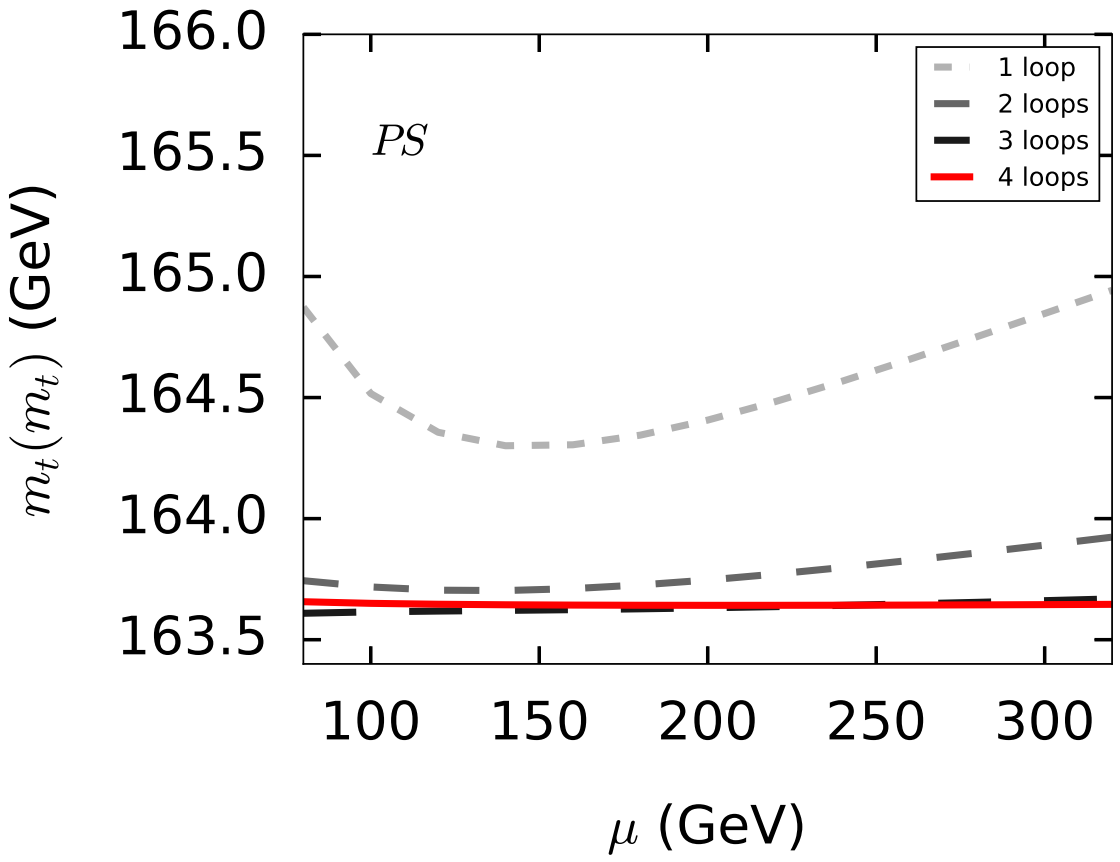

Figure 1: $\overline{\rm MS}$ top quark mass $m_t(m_t)$ computed from the PS mass with LO, NLO, NNLO and N^{3}LO accuracy as a function of the renormalization scale used in the $\overline{\rm MS}$-threshold mass relation.

of uncertainties one ends up in a final uncertainty below 20 MeV which is sufficient for a precise determination of m_t at a future linear collider [34].

Let us at this point have a closer look to the PS mass. In Table 1 the renormalization scale has been fixed to $\mu = m_t$. It is also interesting to consider different values of μ and compute in a first step $m_t(\mu)$ which is then evolved to $m_t(m_t)$ using renormalization group methods. In Figure 1 we

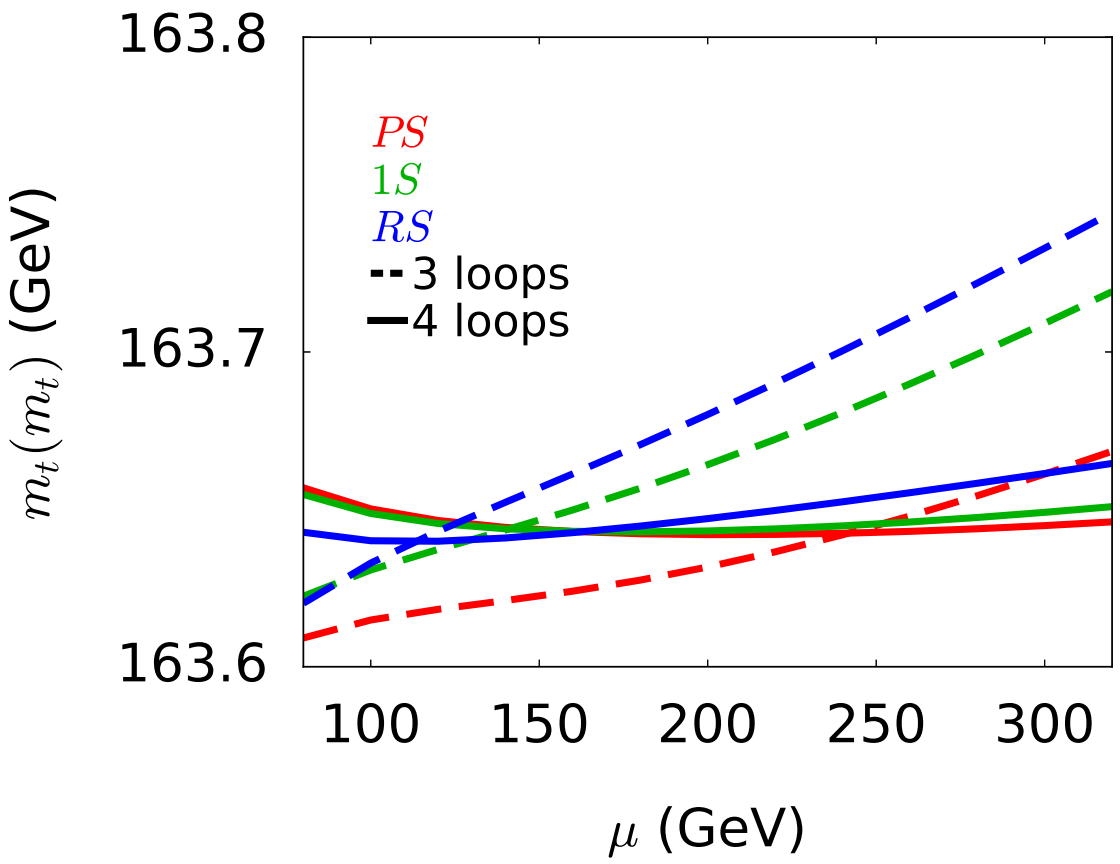

Figure 2: $\overline{\rm MS}$ top quark mass $m_t(m_t)$ computed from the PS, 1S and RS mass with NNLO (dashed) and N^{3}LO (solid line) accuracy as a function of the renormalization scale used in the $\overline{\rm MS}$-threshold mass relation. For $\mu = 300$ GeV the lines from bottom to top correspond to the PS, 1S and RS mass.

plot the result for $m_t(m_t)$ computed from $m_t^{\rm PS} = 168.204$ GeV using LO, NLO, NNLO and N^{3}LO accuracy (from short-dashed to solid lines). Whereas the LO curve shows a variation of several hundred MeV the N^{3}LO is basically independent of μ. Actually, in the considered range from $m_t/2$ to $2m_t$ it varies by less than 20 MeV, a number comparable to the difference between the NNLO and N^{3}LO result at the central scale $\mu = m_t$.

The behaviour of the NNLO and N^{3}LO curve of Figure 1 is magnified in Figure 2 (red curves). In addition the corresponding results are shown for the 1S (green) and RS (blue) mass. In all three cases one observes a significant improvement of the μ dependence when going from NNLO to N^{3}LO. Furthermore, the N^{3}LO curves of all three threshold masses only depend mildly on μ.

In Table 2 results for the $\overline{\rm MS}$ bottom quark mass are shown. They are computed from the PS, 1S and RS masses as given in the first and second row of the table using LO, NLO, NNLO and N^{3}LO accuracy. Similar to the top quark case, one observes a rapid convergence with a shift below 10 MeV from the last perturbative order. A variation of the four-loop $\overline{\rm MS}$-on-shell coefficient leads to a shift of 4 MeV in the $\overline{\rm MS}$ mass.

In Table 3 we show the corresponding results for the $\overline{\rm MS}$ charm quark mass. Even in this case

input	$m^{\rm PS} =$	$m^{\rm 1S} =$	$m^{\rm RS} =$
#loops	4.483	4.670	4.365
1	4.266	4.308	4.210
2	4.191	4.190	4.172
3	4.161	4.154	4.158
4	4.163	4.163	4.163
4 ($\times$1.03)	4.159	4.159	4.159

Table 2: $m_b(m_b)$ in GeV computed from the PS, 1S and RS quark mass using LO to N^{3}LO accuracy. The numbers in the last line are obtained by taking into account the uncertainty of the four-loop coefficient, i.e., it is increased by 3%. The factorization scales for the PS and RS mass are set to 2 GeV.

input	$m^{\rm PS} =$	$m^{\rm 1S} =$	$m^{\rm RS} =$
#loops	1.155	1.552	1.044
1	1.078	1.265	1.028
2	1.021	1.119	1.008
3	0.993	1.033	0.991
4	0.986	0.986	0.986
4 ($\times$1.03)	0.984	0.984	0.984

Table 3: $m_c(3\ {\rm GeV})$ in GeV computed from the PS, 1S and RS quark mass using LO to N^{3}LO accuracy. The numbers in the last line are obtained by taking into account the uncertainty of the four-loop coefficient, i.e., it is increased by 3%. The factorization scales for the PS and RS mass are set to 2 GeV.

we observe a reasonable convergence of the perturbative series. For the PS and RS mass the N^{3}LO corrections are even below 10 MeV.

4. Conclusions

In this contribution we considered the four-loop relation between the $\overline{\rm MS}$ and on-shell heavy quark masses and applied it to the top, bottom and charm case. Whereas the perturbative series converges well for top it does not for the other two cases. This suggests that the on-shell top quark mass is a reasonably good parameter at the order of 100 MeV or even better. For all three cases the perturbative relation between the threshold (PS, 1S, RS) and the $\overline{\rm MS}$ masses is perturbatively well behaved. Thus, in case a threshold mass is determined from a physical quantity like a (threshold) cross section or a bound state energy it can be related to the corresponding $\overline{\rm MS}$ mass with high precision.

Acknowledgments

We thank the High Performance Computing Center Stuttgart (HLRS) and the Supercomputing Center of Lomonosov Moscow State University [35] for providing computing time used for

the numerical computations with FIESTA. P.M. was supported in part by the EU Network HIGGSTOOLS PITN-GA-2012-316704. This work was supported by the DFG through the SFB/TR 9 "Computational Particle Physics". The work of V.S. was supported by the Alexander von Humboldt Foundation (Humboldt Forschungspreis).

References

[1] P. Marquard, A. V. Smirnov, V. A. Smirnov and M. Steinhauser, Phys. Rev. Lett. **114** (2015) 14, 142002 doi:10.1103/PhysRevLett.114.142002 [arXiv:1502.01030 [hep-ph]].

[2] M. Beneke, Phys. Lett. B **434** (1998) 115 [hep-ph/9804241].

[3] A. H. Hoang, Z. Ligeti and A. V. Manohar, Phys. Rev. D **59** (1999) 074017 [hep-ph/9811239].

[4] A. H. Hoang, Z. Ligeti and A. V. Manohar, Phys. Rev. Lett. **82** (1999) 277 [hep-ph/9809423].

[5] A. H. Hoang and T. Teubner, Phys. Rev. D **60** (1999) 114027 [hep-ph/9904468].

[6] A. Pineda, JHEP **0106** (2001) 022 [hep-ph/0105008].

[7] P. A. Baikov, K. G. Chetyrkin and J. H. KÃijhn, JHEP **1410** (2014) 76 doi:10.1007/JHEP10(2014)076 [arXiv:1402.6611 [hep-ph]].

[8] K. G. Chetyrkin, Phys. Lett. B **404** (1997) 161 [hep-ph/9703278].

[9] J. A. M. Vermaseren, S. A. Larin and T. van Ritbergen, Phys. Lett. B **405** (1997) 327 [hep-ph/9703284].

[10] K. G. Chetyrkin, Nucl. Phys. B **710** (2005) 499 [hep-ph/0405193].

[11] R. Tarrach, Nucl. Phys. B **183** (1981) 384.

[12] N. Gray, D. J. Broadhurst, W. Grafe and K. Schilcher, Z. Phys. C **48** (1990) 673.

[13] K. G. Chetyrkin and M. Steinhauser, Phys. Rev. Lett. **83** (1999) 4001 [hep-ph/9907509].

[14] K. G. Chetyrkin and M. Steinhauser, Nucl. Phys. B **573** (2000) 617 [hep-ph/9911434].

[15] K. Melnikov and T. v. Ritbergen, Phys. Lett. B **482** (2000) 99 [hep-ph/9912391].

[16] P. Marquard, L. Mihaila, J. H. Piclum and M. Steinhauser, Nucl. Phys. B **773** (2007) 1 [hep-ph/0702185].

[17] P. Nogueira, J. Comput. Phys. **105** (1993) 279.

[18] J. A. M. Vermaseren, math-ph/0010025.

[19] R. Harlander, T. Seidensticker and M. Steinhauser, Phys. Lett. B **426** (1998) 125 [hep-ph/9712228].

[20] T. Seidensticker, hep-ph/9905298.

[21] S. Laporta, Int. J. Mod. Phys. A **15** (2000) 5087 [hep-ph/0102033].

[22] A. V. Smirnov, Comput. Phys. Commun. **189** (2014) 182 doi:10.1016/j.cpc.2014.11.024 [arXiv:1408.2372 [hep-ph]].

[23] P. Marquard, D. Seidel, unpublished.

[24] A. Pak, J. Phys. Conf. Ser. **368** (2012) 012049 [arXiv:1111.0868 [hep-ph]].

[25] A. V. Smirnov and V. A. Smirnov, Comput. Phys. Commun. **184** (2013) 2820 [arXiv:1302.5885 [hep-ph]].

[26] A. V. Smirnov and M. N. Tentyukov, Comput. Phys. Commun. **180** (2009) 735 [arXiv:0807.4129 [hep-ph]].

[27] A. V. Smirnov, V. A. Smirnov and M. Tentyukov, Comput. Phys. Commun. **182** (2011) 790 [arXiv:0912.0158 [hep-ph]].

[28] A. V. Smirnov, Comput. Phys. Commun. **185** (2014) 2090 [arXiv:1312.3186 [hep-ph]].

[29] K. G. Chetyrkin, J. H. Kühn, A. Maier, P. Maierhofer, P. Marquard, M. Steinhauser and C. Sturm, Phys. Rev. D **80** (2009) 074010 [arXiv:0907.2110 [hep-ph]].

[30] K. A. Olive *et al.* [Particle Data Group Collaboration], Chin. Phys. C **38** (2014) 090001.

[31] K. G. Chetyrkin, J. H. Kühn and M. Steinhauser, Comput. Phys. Commun. **133** (2000) 43 [hep-ph/0004189].

[32] B. Schmidt and M. Steinhauser, Comput. Phys. Commun. **183** (2012) 1845 [arXiv:1201.6149 [hep-ph]].

[33] [ATLAS and CDF and CMS and D0 Collaborations], arXiv:1403.4427 [hep-ex].

[34] M. Beneke, Y. Kiyo, P. Marquard, A. Penin, J. Piclum and M. Steinhauser, Phys. Rev. Lett. **115** (2015) 19, 192001 doi:10.1103/PhysRevLett.115.192001 [arXiv:1506.06864 [hep-ph]].

[35] V. Sadovnichy, A. Tikhonravov, V. Voevodin, and V. Opanasenko, "'Lomonosov': Supercomputing at Moscow State University." In Contemporary High Performance Computing: From Petascale toward Exascale (Chapman & Hall/CRC Computational Science), pp.283-307, Boca Raton, USA, CRC Press, 2013.